Redox Biology 17 (2018) 386–399

Contents lists available at ScienceDirect

Redox Biology

journal homepage: www.elsevier.com/locate/redox

GSNOR modulates hyperhomocysteinemia-induced T cell activation and atherosclerosis by switching Akt S-nitrosylation to phosphorylation

Jing Li[a], Yan Zhang[b], Yuying Zhang[c], Silin Lü[a], Yutong Miao[a], Juan Yang[a], Shenming Huang[a], Xiaolong Ma[a], Lulu Han[a], Jiacheng Deng[a], Fangfang Fan[b], Bo Liu[a], Yong Huo[b], Qingbo Xu[f], Chang Chen[c,d,e,*], Xian Wang[a,*], Juan Feng[a,*]

[a] Department of Physiology and Pathophysiology, School of Basic Medical Sciences, Peking University, Key Laboratory of Molecular Cardiovascular Science, Ministry of Education, 38 Xueyuan Road, Beijing 100191, China
[b] Department of Cardiology, Peking University First Hospital, Beijing 100034, China
[c] National Laboratory of Biomacromolecules, CAS Center for Excellence in Biomacromolecules, Institute of Biophysics, Chinese Academy of Sciences, Beijing 100101, China
[d] University of Chinese Academy of Sciences, Beijing 100049, China
[e] Beijing Institute for Brain Disorders, Capital Medical University, Beijing 100069, China
[f] Cardiovascular Division, BHF Centre for Vascular Regeneration, King's College London, London, UK

ARTICLE INFO

Taxonomy:
Post-Translational Modification
Medical Biology
Oxidoreductase

Keywords:
Hyperhomocysteinemia
Atherosclerosis
GSNOR
T cell
Akt

ABSTRACT

The adaptive immune system plays a critical role in hyperhomocysteinemia (HHcy)-accelerated atherosclerosis. Recent studies suggest that HHcy aggravates atherosclerosis with elevated oxidative stress and reduced S-nitrosylation level of redox-sensitive protein residues in the vasculature. However, whether and how S-nitrosylation contributes to T-cell-driven atherosclerosis remain unclear. In the present study, we report that HHcy reduced the level of protein S-nitrosylation in T cells by inducing S-nitrosoglutathione reductase (GSNOR), the key denitrosylase that catalyzes S-nitrosoglutathione (GSNO), which is the main restored form of nitric oxide *in vivo*. Consequently, secretion of inflammatory cytokines [interferon-γ (IFN-γ) and interleukin-2] and proliferation of T cells were increased. GSNOR knockout or GSNO stimulation rectified HHcy-induced inflammatory cytokine secretion and T-cell proliferation. Site-directed mutagenesis of Akt at Cys224 revealed that S-nitrosylation at this site was pivotal for the reduced phosphorylation at Akt Ser473, which led to impaired Akt signaling. Furthermore, on HHcy challenge, as compared with $GSNOR^{+/+}ApoE^{-/-}$ littermate controls, $GSNOR^{-/-}ApoE^{-/-}$ double knockout mice showed reduced T-cell activation with concurrent reduction of atherosclerosis. Adoptive transfer of $GSNOR^{-/-}$ T cells to $ApoE^{-/-}$ mice fed homocysteine (Hcy) decreased atherosclerosis, with fewer infiltrated T cells and macrophages in plaques. In patients with HHcy and coronary artery disease, the level of plasma Hcy was positively correlated with *Gsnor* expression in peripheral blood mononuclear cells and IFN-γ^+ T cells but inversely correlated with the S-nitrosylation level in T cells. These data reveal that T cells are activated, in part *via* GSNOR-dependent Akt denitrosylation during HHcy-induced atherosclerosis. Thus, suppression of GSNOR in T cells may reduce the risk of atherosclerosis.

1. Introduction

Atherosclerosis is a chronic inflammatory disease characterized by lipid and leukocyte accumulation within the arterial wall. Homocysteine (Hcy) is a thiol-containing amino acid derivative derived from the metabolism of dietary methionine. Epidemiological studies have shown that elevated plasma level of Hcy, known as hyperhomocysteinemia (HHcy), is an independent risk factor for atherosclerosis [1–3]. Our previous studies indicated that HHcy accelerates atherosclerotic development in apolipoprotein E-deficient ($ApoE^{-/-}$) mice [4] and T-cell activation, with elevated reactive oxygen species (ROS) production and promoted proliferation, plays an important role in this process [5–7]. Recent studies suggest that HHcy promotes atherosclerosis in $ApoE^{-/-}$ mice by reducing S-nitrosylated

Abbreviations: ApoE, apolipoprotein E; CAD, coronary artery disease; DTT, dithiothreitol; GSNO, S-nitrosoglutathione; GSNOR, S-nitrosoglutathione reductase; Hcy, homocysteine; HHcy, hyperhomocysteinemia; IFN-γ, interferon γ; IL-2, Interleukin 2; iNOS, inducible nitric oxide synthase; NAc, N-acetyl-L-cysteine; NO, nitric oxide; PBMC, peripheral blood mononuclear cell; ROS, reactive oxygen species; SNO-protein, S-nitrosylated protein; SNOs, S-nitrosothiols

* Corresponding authors.
E-mail addresses: changchen@moon.ibp.ac.cn (C. Chen), xwang@bjmu.edu.cn (X. Wang), juanfeng@bjmu.edu.cn (J. Feng).

https://doi.org/10.1016/j.redox.2018.04.021
Received 1 April 2018; Received in revised form 24 April 2018; Accepted 28 April 2018
Available online 01 May 2018

protein (SNO-protein) levels in the aorta, and causes significant reduction of protein S-nitrosylation accompanied by increasing ROS in vascular endothelial cells [8,9].

Substantial evidence indicates accumulation of ROS provides microenvironment within cells for altering the reversible nitrosative modification level of redox-sensitive residues in proteins [10]. S-nitrosylation, the covalent addition of an NO group to a reactive free thiol of proteins to form S-nitrosothiols (SNOs), is emerging as a critical reversible post-translational modification involved in the regulation of T-cell functions [11,12]. The regulation of S-nitrosylation/denitrosylation, being as a redox switch, depends on several key enzymes, such as nitric oxide synthases (NOS) and denitrosylases [13]. S-nitrosoglutathione (GSNO) reductase (GSNOR) is the enzyme that metabolizes GSNO, a major physiological NO derivative, thus regulating the equilibrium between SNO-proteins and GSNO [14]. Genetic deletion of GSNOR in mice causes excessive protein S-nitrosylation, increased apoptosis and reduced number of T cells in the thymus [15], which indicates a protective role of GSNOR in T-cell development *via* regulation of S-nitrosylation. However, whether GSNOR-induced denitrosylation contributes to T cell activation and atherosclerotic development remains unknown.

Over the years, multiple T-cell functions in response to S-nitrosylation have become increasingly recognized. SNO-proteins, such as the caspase family (−1, −3, −8), NF-κB and Bcl-2, are key regulators in T-cell apoptosis [16–19]. During immunization, NO produced by inducible nitric oxide synthase (iNOS) suppresses the survival of T cells to control the persistence of $CD4^+$ and $CD8^+$ T-cell immune memory [20]. Moreover, accumulating evidence suggests a protective role of S-nitrosylation in various autoimmune diseases by modulating the differentiation of T helper (Th) cell subsets, including Th-1, − 2 and − 17 [11]. These previous studies indicated the direct or indirect regulatory effects of S-nitrosylation on T-cell apoptosis, survival, differentiation and development, but the regulatory effects of S-nitrosylation on Hcy-induced primary T-cell activation, including cytokine secretion and proliferation, remain to be fully elucidated.

Our previous work showed that HHcy promotes Akt phosphorylation in T cells to accelerate atherosclerosis [6]. The phosphoinositide-3 kinase (PI3K)/Akt pathway is critical for regulating T-cell proliferation, metabolism, cytokine production and survival [21–23]. Upon activation, naïve T cells develop into T_{eff} cells that enter the bloodstream and are recruited into atherosclerotic plaques, where they proliferate and produce proinflammatory cytokines [24]. Recent reports have shown that Akt can be S-nitrosylated in muscle cells and esophageal squamous cells, leading to its inhibited kinase activity in diabetic models, post-burn injury, and squamous cell differentiation [25–27]. Considering the crucial role of Akt-mediated T-cell activation in HHcy-accelerated atherosclerosis, whether and how S-nitrosylation of Akt regulates Hcy-induced T-cell activation and the mechanism underlying the intracellular pathway remain to be determined.

In this study, we demonstrate that HHcy upregulated the expression of GSNOR in T cells. As a result, GSNOR induced denitrosylation of Akt in Hcy-activated T cells *in vivo* and *in vitro*, which contributed to vascular inflammation and susceptibility to atherosclerosis in $GSNOR^{-/-}ApoE^{-/-}$ mice. The translational implication of the current study builds on the positive correlation between GSNOR-dependent denitrosylation in T cells and the development of HHcy-induced coronary heart disease (CAD) in humans.

2. Material and methods

2.1. Mice and animal models

C57BL/6 J mice and $ApoE^{-/-}$ mice were purchased from the Animal Center of Peking University Health Science Center (Beijing, China). GSNOR-deficient ($GSNOR^{-/-}$) mice on a C57BL/6 J background were provided by Dr. Limin Liu (University of California, San Francisco), and $GSNOR^{-/-}ApoE^{-/-}$ mice were generated by crossing $GSNOR^{-/-}$ mice and $ApoE^{-/-}$ mice (both on a C57BL/6 J background) in our laboratory. All mice were maintained under specific pathogen-free conditions. Mice were randomly divided into different treated groups without any preference, and body weight was measured before the experiment to ensure no significant differences among groups. To induce HHcy in mice, the different types of mice aged 6 weeks were fed a normal mouse chow diet and drinking water supplemented with or without 1.8 g/L Hcy (Sigma-Aldrich, St. Louis, MO, USA) for 4 weeks as previously described [4]. For adoptive T-cell transfer experiments, 5-week-old $ApoE^{-/-}$ mice as recipients were treated intraperitoneally with 4.5 μg/mouse anti-mouse CD3ε $F(ab')_2$ fragment (145–2C11; Bio X Cell, West Lebanon, NH) (the CD3 blockade antibody) for 7 consecutive days to block innate T cells as previously described [28,29]. The recipients then rested for 3 days before caudal vein injection with T cells (2×10^7 cells/mouse) that were freshly isolated from $GSNOR^{+/+}$ or $GSNOR^{-/-}$ mice. After T-cell transfer, recipient mice were fed a normal chow diet and drinking water with or without 1.8 g/L Hcy for 3 weeks. All studies were performed according to protocols approved by the Committee on the Ethics of Animal Experiments of Peking University Health Science Center and conform to the guidelines from Directive 2010/63/EU of the European Parliament on the protection of animals used for scientific purposes or the National Institutes of Health guidelines. All animal experiments were conducted according to the Animal (Scientific Procedures) Act of 1986 (UK).

2.2. Clinical samples and study design

All clinical samples were obtained at Peking University First Hospital with informed consent and ethical review committee approval (protocol no. 2017.03.22). All experiments were conducted according to the principles expressed in the Declaration of Helsinki. Patients with CAD and HHcy (plasma Hcy above 10 μmol/L) were recruited (n = 18) for the study. The baseline characteristics of patients are summarized (Supplementary Table 3). The level of plasma Hcy was detected by using an ARCHITECT i2000SR analyzer (Abbott Laboratories Philippines, Taguig City, Philippines). Human peripheral blood mononuclear cells (PBMCs) were isolated from 5 mL heparin-anticoagulated venous blood by Ficoll-Paque gradient centrifugation. For quantification of the SNO-cysteine (SNO-Cys) level in $CD3^+$-gated T cells and mRNA level of *Gsnor* in PBMCs, PBMCs (1×10^6 and 5×10^6 cells) were collected for flow cytometry and RNA extraction, respectively, after isolation. To quantify the proportion of IFN-γ^+ T cells, 1×10^6 PBMCs were suspended in RPMI 1640 medium (Gibco, Gaithersburg, MD, USA) supplemented with 10% fetal bovine serum (Gemini Bio-Products, West Sacramento, CA, USA). PMA and ionomycin (Sigma-Aldrich, St. Louis, MO, USA) were added at 100 ng/mL and 1 μg/mL, respectively, for 12 h, and a 1000 × brefeldin A solution (420601, Biolegend, San Diego, CA, USA) was added per the instructions 4 h before harvest. CD3, SNO-Cys and IFN-γ were stained and analyzed by flow cytometry as described below.

2.3. Cell isolation and culture

Splenic T cells were isolated from mice and purified by positive selection with magnetic microbeads against CD90.2 (Miltenyi Biotec, Bergisch Gladbach, Germany) following the manufacturer's protocol. Purified T cells were cultured in RPMI 1640 medium (Gibco, Gaithersburg, MD, USA) supplemented with 10% fetal bovine serum (Gemini Bio-Products, West Sacramento, CA, USA) in cell culture plates containing plate-bound anti-CD3 antibody (1 μg/mL, BD Pharmagen, Franklin Lakes, NJ, USA). Purified T cells were further treated with or without 100 μmol/L Hcy for the indicated times. Under some conditions, T cells were pretreated with 50 μmol/L GSNO (provided by Prof. C Chen) or S-nitrosylation inhibitors, 50 μmol/L N-acetyl-L-cysteine (NAc, Sigma Aldrich) or 25 μmol/L dithiothreitol (DTT) for 30 min, and

then incubated together with or without 100 μmol/L Hcy for the indicated times.

2.4. Detection of protein S-nitrosylation with the irreversible biotinylation procedure (IBP)

Protein S-nitrosylation was detected with the IBP, as previously described [30], which is an improved method based on the original biotin switch assay [31].

2.5. Quantitative S-nitrosylation proteomics and data analysis

The iodoTMT labeling was conducted by using iodoacetyl tandem mass tag™ (iodoTMT™) reagents (90103, Thermo Scientific, USA) as described by Qu *et al.* [32] Briefly, isolated splenic T cells were lysed in HENS buffer, free cysteines were blocked with methyl methanethiosulfonate (MMTS), and S-nitrosylated cysteines were labeled with iodoTMT reagent and enriched with anti-TMT antibody. Peptides were finally eluted and resuspended in 5% acetonitrile/0.1% formic acid. The multiplexed quantitative mass spectrometry data were collected by using Q Exactive mass spectrometer equipped with an easy n-LC 1000 HPLC system (Thermo Scientific) on data-dependent acquisition mode. The raw data from Q Exactive were analyzed with Proteome Discovery version 1.4 using Sequest HT search engine for protein identification and Percolator for false discovery rate analysis. The Uniprot mice protein database was used for searching data from the mice sample. Protein quantification was also performed on Proteome Discovery version 1.4 using the ratio of the intensity of reporter ions from the MS/MS spectra. Only unique peptides of proteins or protein groups were selected for protein relative quantification. The total SNO-Proteins of $GSNOR^{+/+}$ mice fed regular drinking water were considered as control reference for calculating the ratios among groups. The normalization to the protein median of each sample was used to corrected experiment bias.

2.6. ELISA

For analysis of cell culture supernatants, T cells (1×10^6 cells/well) were seeded in a 48-well plate for 24 h, and supernatants from the cell cultures were harvested. The interleukin (IL-2) and interferon-γ (IFN-γ) levels of the supernatants (diluted 1:1 for IL-2 and 1:30 for IFN-γ) were analyzed and quantified by using a mouse-specific ELISA kit (NeoBioscience Technology, Shenzhen, China).

2.7. Enzyme activity assays

For Akt enzyme activity analysis, we used an Akt/PKB kinase activity measurement kit (Baomanbio, Shanghai). The final reaction volume was 200 μL, and reactions were performed in 96-well plates. The decrease in absorbance after the addition of NADH at 340 nm was monitored and measured to determine Akt kinase activity by using a Varioskan Flash Multimode Reader (Thermo Fisher Scientific, Waltham, MA, USA). For Akt signaling network analysis, we used an Akt signaling antibody array kit (#9700, Cell Signaling Technology, Danvers, MA, USA).

2.8. Flow cytometry

Plasma inflammatory cytokine levels were investigated by using a cytometric bead array inflammation kit (BD Biosciences, San Jose, CA, USA). For measure of T cell proportion in CD3-blockade-treated mice, the lymphatic node cells and splenic cells were stained with PE anti-mouse CD3 antibody diluted in PBS. For measure of SNO-Cys MFI in T cells and IFN-γ^+ T cell proportion, the human PBMCs were stained with surface marker FITC anti-human CD3 antibody diluted in PBS. The samples were washed with PBS after surface staining, fixed and permeabilized with Foxp3/Transcription Factor Staining Buffer Set according to the manufacturer's instructions (00–5523–00, eBioscience, CA, USA), then stained with APC anti-human IFN-γ antibody or anti-SNO-Cys antibody. Subsequently, Alexa Fluor 555-labeled secondary antibody were used to label SNO-Cys in cells. The data was analyzed by flow cytometry with Cell QuestPro software (BD Biosciences, USA). The $CD3^+$ T cell gate was identified and the proportion of IFN^+ cells and the MFI of Alexa Fluor 555 secondary-labeled SNO-Cys in gated $CD3^+$ T cells were analyzed by FlowJo software (Tree Star, Ashland, OR, USA).

2.9. CFSE staining and cell proliferation

Purified T cells were stained with 1 μmol/L CFSE (Invitrogen, Carlsbad, CA, USA) for 5 min at room temperature in the dark and washed twice with PBS supplemented with 5% fetal bovine serum. Stained cells were cultured for 48 h and analyzed by flow cytometry. The data were analyzed by using FlowJo software.

2.10. Western blot analysis

Cell or tissue extracts containing equal amounts of total protein were resolved with 10% SDS-polyacrylamide gel electrophoresis and transferred to nitrocellulose membranes, which were blocked with 5% bovine serum albumin for 1 h and incubated with various antibodies at 4 °C overnight, then IRDye 700- or 800-conjugated secondary antibodies (1:20000, Rockland, Gilbertsville, PA, USA) for 1 h at room temperature. The fluorescence signal was detected and analyzed by using an Odyssey infrared imaging system (LI-COR Biosciences, Lincoln, NE, USA).

2.11. Antibodies

Flow cytometry was performed with PE anti-mouse CD3 antibody (#555275, 1:200), FITC anti-human CD3 (#555332, 1:10), APC anti-human IFN-γ (#551385, 1:200) from BD Biosciences (San Jose, CA, USA), anti-SNO-cys (N5411, 1:200, Sigma-Aldrich, St. Louis, MO, USA), and Alexa Fluor 555-labeled goat anti-rabbit secondary antibody (1:400, A32732, Invitrogen, Carlsbad, CA, USA).

Antibodies for western blot analysis included anti-phospho-Akt (Ser473), anti-phospho-Akt (Thr308), anti-Akt, anti-β-actin, anti-GAPDH, anti-flag (1:1000, all from Cell Signaling Technology, Danvers, MA, USA), anti-SNO-Cys (1:1000, Sigma-Aldrich, St. Louis, MO, USA), anti-iNOS (1:500, Santa Cruz Biotechnology, Santa Cruz, CA, USA), anti-Trx1 (1:1000, ABclonal Biotechnology, Hubei, China), and anti-GSNOR (1:1000, Proteintech, Rosemont, USA).

2.12. Quantitative RT-PCR

Cells and aortas were collected, and total RNA was extracted by the TRIzol reagent method (Invitrogen, Carlsbad, CA, USA), then reverse-transcribed to cDNA and amplified using the AMV Reverse Transcription System (Promega, Madison, WI, USA). All amplification reactions involved the use of the Mx3000 Multiplex Quantitative PCR System (Stratagene, La Jolla, CA, USA). The primer sequences used for PCR analyses based on mouse genes were as follows: *Il-2* (forward, CAGGAACCTGAAACTCCCCA; reverse, AGAAAGTCCACCACAGTTGC), *Ifn-γ* (forward, TGGCTGTTTCTGGCTGTTAC; reverse, TTCGCCTTGCT GTTGCTGAAG), *Gsnor* (forward, TATTTCAACTGGCTACGG; reverse, CTCAAGGGCTGATCTCAT), *iNos* (forward, AAACGCTTCACTTCCAATG; reverse, CAATCCACAACTCGCTCC), *Icam-1* (forward, AGCTCGGAGGA TCACAAA; reverse, TCTGCTGAGACCCCTCTTG), *Vcam-1* (forward, CTGTTCCAGCGAGGGTCTA; reverse, CACAGCCAATAGCAGCACA), *Tnf-α* (forward, ACAGAAAGCATGATCCGCGAC; reverse, CCGATCACC CCGAAGTTCAGTA), *Mcp-1* (forward, CAGATGCAGTTAACGCCC; reverse, ATTCCTTCTTGGGGTCAGC), *Il-10* (forward, TGTCAAATTCATT CATGGCCT; reverse, ATCGATTTCTCCCCTGTGAA), *β-Actin* (forward,

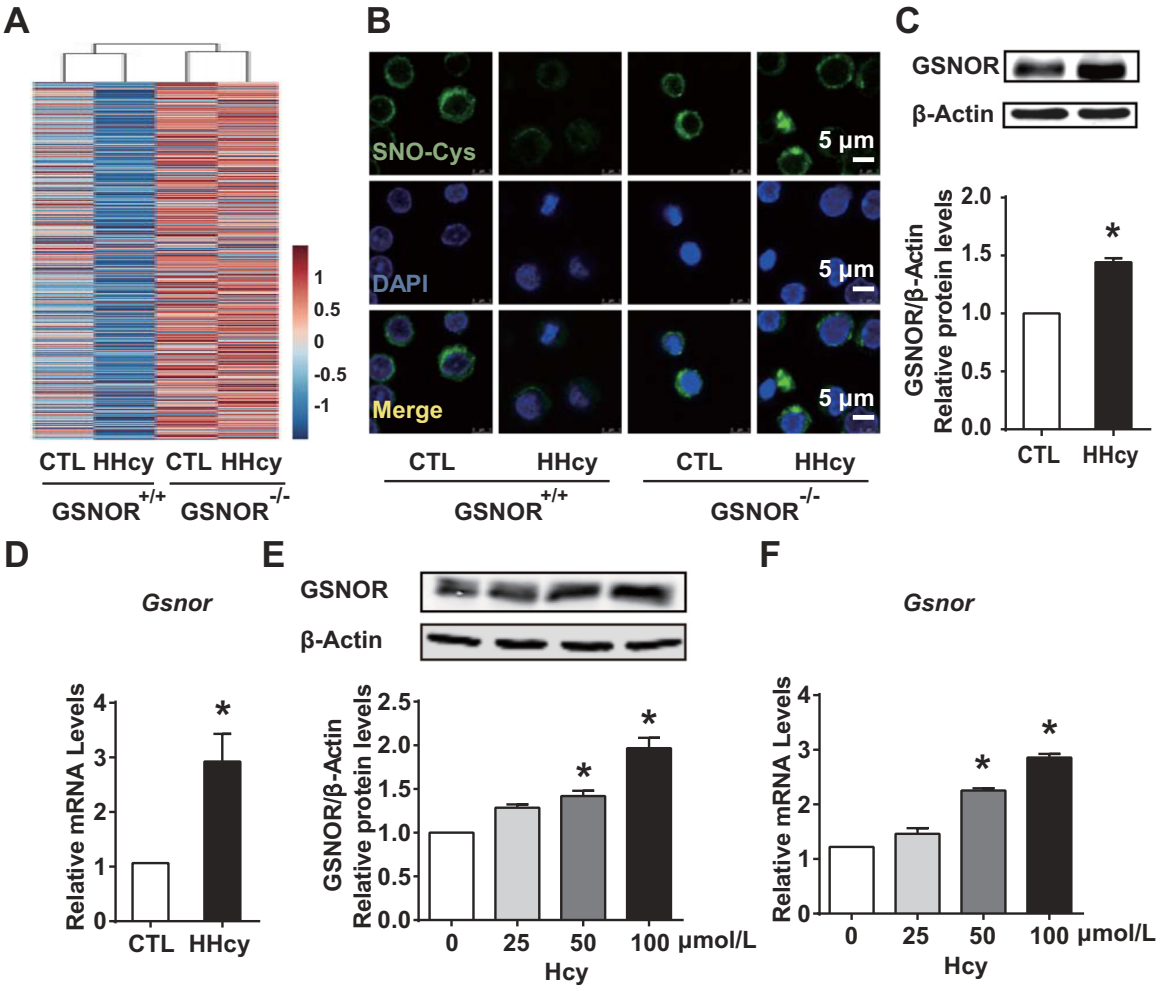

Fig. 1. Hyperhomocysteinemia (HHcy) reduces S-nitrosylation levels by upregulating S-nitrosoglutathione reductase (GSNOR) in T cells. (*A-B*), GSNOR-deficient ($GSNOR^{-/-}$) mice or $GSNOR^{+/+}$ wild-type littermates were fed a normal chow diet and given drinking water supplemented with or without 1.8 g/L homocysteine (Hcy) for 4 weeks. Splenic T cells were purified from control or HHcy mice. (*A*), S-nitrosylated proteins (SNO-Proteins) in T cells were labeled with iodoTMT™ and subjected to LC-MS/MS-based proteiomics. (*B*), Representative fluorescence confocal images of T cells stained with anti-SNO-Cys (green) and DAPI (blue) to highlight nuclei. (*C-D*), C57BL/6 J mice fed a normal chow diet and given drinking water supplemented with or without 1.8 g/L homocysteine (Hcy) for 4 weeks. Splenic T cells were purified from control or HHcy mice. (*E-F*), Splenic T cells purified from C57BL/6 J mice cultured and incubated with different levels of Hcy (0, 25, 50, 100 μmol/L) for 24 h *in vitro*. (*C, E*), Western blot analysis of GSNOR protein expression and quantification. β-Actin was an internal control. (*D, F*), Gene expression of *Gsnor* measured by quantitative PCR in T cells. Data are mean ± SEM of at least three independent experiments (n = 3–6 mice in each group). * P <.05 compared with the control.

GTGACGTTGACATCCGTAAAGA; reverse, GCCGGACTCATCGTACTCC). The primer sequences based on human genes are as follows: *Gsnor* (forward, ATGGCGAACGAGGTTATCAAG; reverse, CATGTCCCAAGAT CACTGGAAAA).

2.13. Plasmid construction and transfection

Mouse Akt-WT was amplified from T-cell cDNA with primers containing 5′ *Eco*RI and 3′ *Xba*I restriction sites, and the PCR product and 3 × flag-pCMV vector were cut and ligated. Cysteine-to-serine mutants (Akt-C224S, C296S) were constructed by using the fast mutagenesis kit (TransGen Biotech, Beijing). Various Akt plasmids were transfected into EL4 cells by using an Amaxa Cell Line Necleofector kit (Lonza Cologne GmbH, Cologne, Germany) according to the manufacturer's protocol.

2.14. Protein expression and purification

The *Akt* gene was ligated into the pET-28a(+) expression plasmid for protein expression. The construct for Akt was provided by Synbio Tech (ID: CN5905-2, Suzhou, China). The Akt protein was produced in BL21(DE3) *E. coli* cells, induced with 0.1 mmol/L isopropyl 1-thio-β-D-galactopyranoside, and grown at 16 °C for 16 h. The harvested cells were lysed by using PBS buffer (pH 7.4), and the debris was removed by centrifugation (12,000 rpm, 1 min). The supernatant was then loaded onto Ni sepharose (17–5318–01, Ni sepharose 6 fast flow, GE healthcare, USA) and washed with PBS buffer containing 50 mmol/L imidazole (pH 7.4). Proteins were eluted by using PBS buffer containing 200 mmol/L imidazole. The excessive imidazole was removed by equilibrium dialysis *via* semipermeable membranes.

2.15. Circular dichroism and secondary structure analysis

Far-UV circular dichroism (CD) spectra were acquired between 200 and 260 nm on a Chirascan Plus CD instrument (Applied Photophysics, UK) at 25 °C in a 0.1-mm-path length thermostated quartz cuvette. Spectra of 0.2 mg/mL Akt protein were measured in PBS buffer with or without GSNO (250 μmol/L). The spectral interference from GSNO in GSNO-treated groups was subtracted by background correction. The secondary structures were assigned by using the CDNN program.

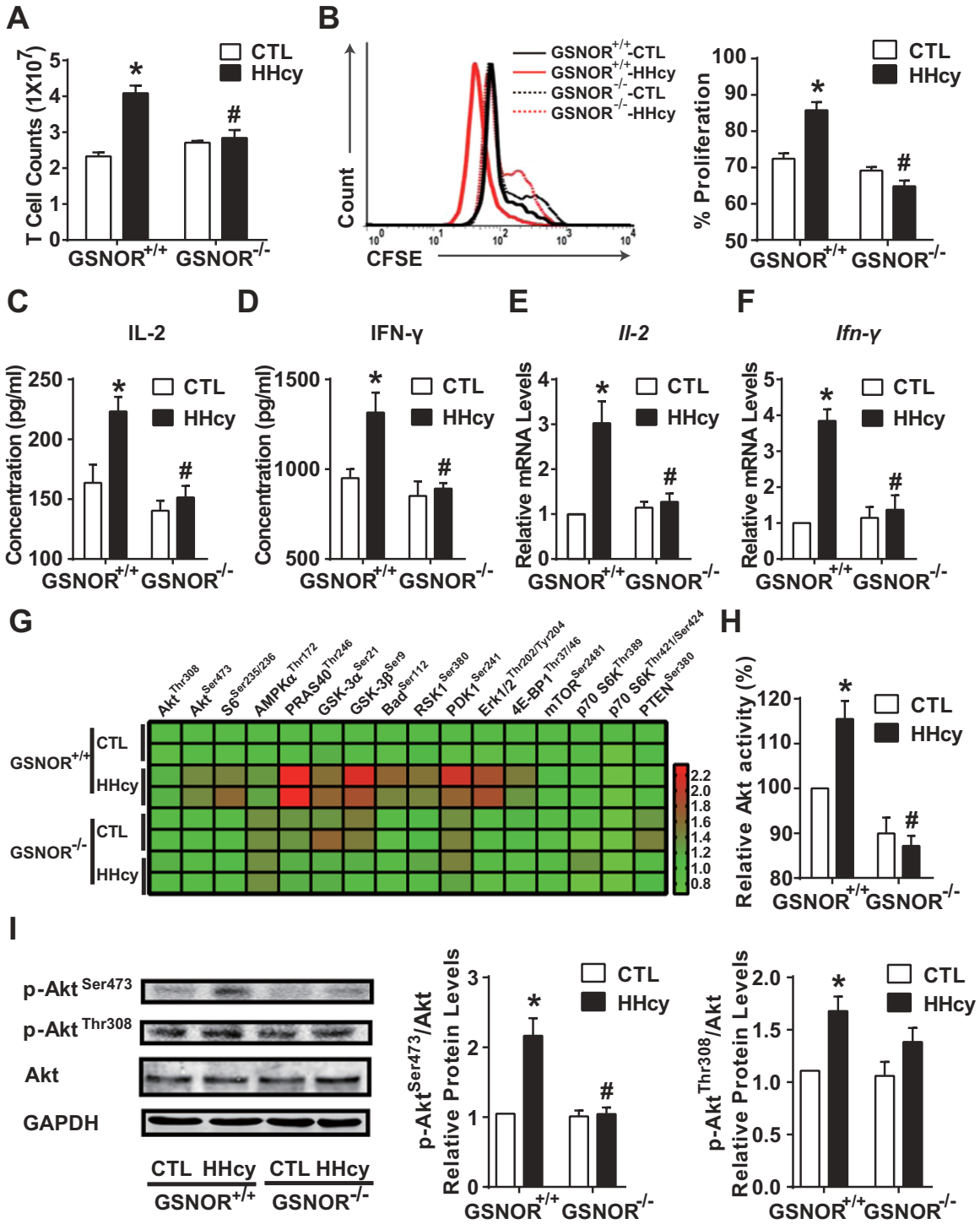

Fig. 2. HHcy activation of T cells depends on GSNOR-Akt axis. GSNOR$^{-/-}$ mice or GSNOR$^{+/+}$ littermates were fed a normal chow diet and given drinking water supplemented with or without 1.8 g/L Hcy for 4 weeks. (*A*), Total cell numbers of splenic T cells. (*B*), Purified T cells were labeled with CFSE before culture with plate-bound anti-CD3 antibody, then cell proliferation was assessed by flow cytometry after 48 h. (*C-D*), Purified T cells were cultured for an additional 24 h with plate-bound anti-CD3 antibody. ELISA of interleukin 2 (IL-2) (*C*) and interferon-γ (IFN-γ) (*D*) levels in supernatants of cultured T cells. (*E-I*), In freshly isolated splenic T cells, gene expression of *Il-2* (*E*) and *Ifn-γ* (*F*) measured by quantitative PCR. Phosphorylated proteins in Akt signaling networks (*G*) were simultaneously detected by using the Akt signaling antibody array kit and presented as a heat map. Akt kinase enzyme activity (*H*) was analyzed, and phosphorylation of Akt at Ser473 and Thr308 (*I*) was detected by western blot analysis. GAPDH was an internal control. Data are mean ± SEM of at least three independent experiments (n = 3–6 mice in each group). * P<.05 compared with the control. $^{\#}P$<.05 compared with HHcy.

2.16. Analysis of atherosclerotic lesions

Hearts were fixed, and frozen aortic root sections (7 μm) were collected on glass slides for Oil-red O and immunofluorescence staining, as described [4]. For immunofluorescence staining, aortic root sections were incubated with primary anti-CD68, anti-SNO-Cys or anti-CD3 antibody, and further stained with fluorescence-conjugated secondary antibodies. The fluorescence signals were measured by confocal laser

scanning microscopy (Leica, Germany). The frozen aortic root sections were prepared by a professional technician, and the immunofluorescence staining was analyzed blindly by another investigator.

2.17. Lipid profile

Plasma total cholesterol and triglyceride levels were assayed by using kits from Zhong Sheng Bio-technology (Beijing).

2.18. Statistical analysis

All data are presented as mean ± SEM unless otherwise stated. Comparisons of data involved unpaired Student *t*-tests for comparing two groups and one-way ANOVA followed by the Newman-Keuls post-hoc test for multiple groups. Statistical analyses involved using GraphPad Prism (La Jolla, CA, USA). Correlational analyses involved Pearson correlation after determining the normal distribution of the data. $P < 0.05$ was considered statistically significant for all experiments.

3. Results

3.1. HHcy reduces S-nitrosylation levels by upregulating GSNOR expression in T cells

To gain insight into whether GSNOR, a key enzyme controlling denitrosylation, is involved in the HHcy regulation of S-nitrosylation in T cells *in vivo*, we administered GSNOR$^{+/+}$ wild-type mice and their GSNOR$^{-/-}$ littermates (both on a C57BL6/J background) with or without Hcy (1.8 g/L) in drinking water for 4 weeks. Plasma Hcy concentrations were higher with than without Hcy in drinking water (Supplementary Table 1). Body weights and total cholesterol and triglyceride levels were not changed among all groups (Supplementary Table 1). By implementing an iodoTMT™ labeling strategy to quantify SNO-proteins, we found the level of SNO-protein in T cells was greatly denitrosylated after HHcy administration in GSNOR$^{+/+}$ mice. However, this reduced protein S-nitrosylation was not seen in T cells from the GSNOR$^{-/-}$ mice (Fig. 1A). Similar changes of SNO-protein levels among groups were observed by using biotin switch assay (Supplementary Fig. 1). We confirmed a marked reduction in SNO-Cys protein content in HHcy-activated wild-type, but not GSNOR-deficient T cells on immunofluorescent images of isolated T cells stained with anti-SNO-Cys antibody (Fig. 1B).

Given the decrease in S-nitrosylation in T cells caused by HHcy, we next determined the expression of GSNOR in T cells. The protein and mRNA expression of GSNOR were markedly upregulated in T cells from HHcy-fed wild-type mice (Fig. 1C, D). Furthermore, in cultured splenic T cells, Hcy stimulation (50, 100 μmol/L) for 24 h dose-dependently upregulated GSNOR protein and mRNA expression (Fig. 1E, F). In addition to upregulated GSNOR transcription, the cellular level of protein S-nitrosylation can be affected by NOS and other denitrosylases [12,13]. Hcy administration *in vivo* and treatment of T cells *in vitro* did not significantly change the protein and mRNA levels of iNOS or Trx (Supplementary Fig. 2A-F). Thus, results in Fig. 1 demonstrate that HHcy increases the expression of GSNOR, leading to decreased SNO-protein levels in T cells.

3.2. HHcy activation of T cells depends on GSNOR-Akt axis

We next explored the role of HHcy-induced GSNOR in T-cell proliferation. First, 4-week HHcy administration elevated T-cell numbers in GSNOR$^{+/+}$ wild-type mice, but not GSNOR$^{-/-}$ littermates (Fig. 2A). Second, HHcy promoted T-cell proliferation to a large extent in GSNOR$^{+/+}$ T cells, which was lacking in GSNOR$^{-/-}$ mice, as revealed by CFSE staining and flow cytometry (Fig. 2B). Together, Figs. 2A and 2B suggest a stimulatory effect of GSNOR on HHcy-induced T-cell proliferation. HHcy stimulated the secretion and gene expression of interleukin 2 (IL-2) and interferon γ (IFN-γ) in GSNOR$^{+/+}$ T cells but not GSNOR$^{-/-}$ T cells (Fig. 2C-F). Cytometric bead array analysis showed lower plasma levels of inflammatory cytokines (*e.g.* TNF-α, IFN-γ, and IL-12p70) in GSNOR$^{-/-}$ than GSNOR$^{+/+}$ mice by HHcy stimulation (Supplementary Table 1). These results indicate that GSNOR is a potent regulator of Hcy-induced T-cell proliferation and activation.

Activated by co-stimulation of T-cell surface receptors, Akt is a key kinase that contributes to various T-cell activation responses [21–24,33]. Because Hcy promotes the PI3K-Akt axis in T cells [6], we then investigated whether Akt is engaged in the GSNOR-dependent T-cell activation by detecting 16 putative phosphorylated proteins predominantly belonging to the Akt signaling network. An Akt signaling antibody array kit was used. The heat map in Fig. 2G showed greater phosphorylation of Akt signaling nodes (*e.g.*, PRAS40^{Thr246}, GSK-3β^{Ser9}) in cell lysates from HHcy-treated GSNOR$^{+/+}$ than GSNOR$^{-/-}$ T cells. Results from this array-based assay suggest that GSNOR was necessary for the activation of HHcy-activated Akt signaling network in T cells. Additionally, the kinase activity of Akt was induced in HHcy-treated GSNOR$^{+/+}$ than GSNOR$^{-/-}$ T cells (Fig. 2H). Akt activation is initiated by its phosphorylation modification at Ser473 and Thr308 [34,35]. Consistently, HHcy induced phosphorylation of Akt at Ser473 and Thr308 in GSNOR$^{+/+}$ T cells and elevated p-Akt^{Ser473}, but not p-Akt^{Thr308}, was diminished in GSNOR$^{-/-}$ T cells (Fig. 2I).

As the substrate of GSNOR, GSNO acts as a major endogenous NO donor. To further confirm the involvement of GSNOR and Akt in T-cell activation under HHcy, we incubated GSNOR$^{+/+}$ splenic T cells with GSNO followed by Hcy treatment. In agreement with results in Fig. 2, GSNO (50 μmol/L) significantly inhibited the Hcy-stimulated T-cell proliferation (Supplementary Fig. 3A) and production of IL-2 and IFN-γ (Supplementary Fig. 3B-E). As well, Hcy-induced Akt activity was attenuated (Supplementary Fig. 3F-H). Taken together, HHcy activated Akt and Akt-elicited signaling pathways by inducing GSNOR. As a result, the HHcy-promoted T-cell proliferation and activation depended on GSNOR and Akt.

3.3. S-Nitrosylation of Akt at Cys224 inhibits the phosphorylation of Akt at Ser473

Akt is a target of S-nitrosylation [25–27]. Because GSNOR deficiency impaired the HHcy-induced p-Akt^{Ser473} *in vivo* and *in vitro*, we examined the causative effect of GSNOR-mediated Akt denitrosylation leading to Akt activation. We used a biotin switch assay to assess Akt S-nitrosylation in T cells from GSNOR$^{+/+}$ and GSNOR$^{-/-}$ littermates. Akt was S-nitrosylated (SNO-Akt) in GSNOR$^{+/+}$ T cells and denitrosylated with HHcy stimulation (Fig. 3A). Intriguingly, the HHcy-dampened Akt S-nitrosylation was restored in GSNOR$^{-/-}$ T cells (Fig. 3A). Similar results were seen in cultured T cells treated with Hcy and GSNO (Fig. 3B).

Although the inhibitory effects of NO donors on Akt phosphorylation were previously reported [26], the interaction between S-nitrosylation and phosphorylation of Akt remained to be addressed. We further treated T cells with the S-nitrosylation inhibitor N-acetyl-L-cysteine (NAc) (50 μmol/L) or dithiothreitol (DTT) (25 μmol/L) in the presence of Hcy and GSNO. NAc and DTT reversed the level of p-Akt^{Ser473}, but not p-Akt^{Thr308}, to a level comparable to the Hcy group despite the presence of GSNO (Fig. 3C, D), which suggests that NAc and DTT could abolish the reduced p-Akt^{Ser473} caused by S-nitrosylation of Akt. These results indicate that S-nitrosylation of Akt impairs its phosphorylation.

Conserved Cys residues within 8 Å of annotated active sites of Akt1 (179 K, 274D) are Cys224, Cys296 and Cys310, as indicated by using PyMOL software, with Cys224 and Cys296 as possible S-nitrosylated Cys residues [25,26]. Therefore, we generated two expression plasmids encoding flag-labeled Akt variants with Cys224 or Cys296 substituted by Ser. These Akt variant plasmids were transfected into EL4 cell lines. On biotin switch assay, S-nitrosylation of wild-type and C296S Akt was

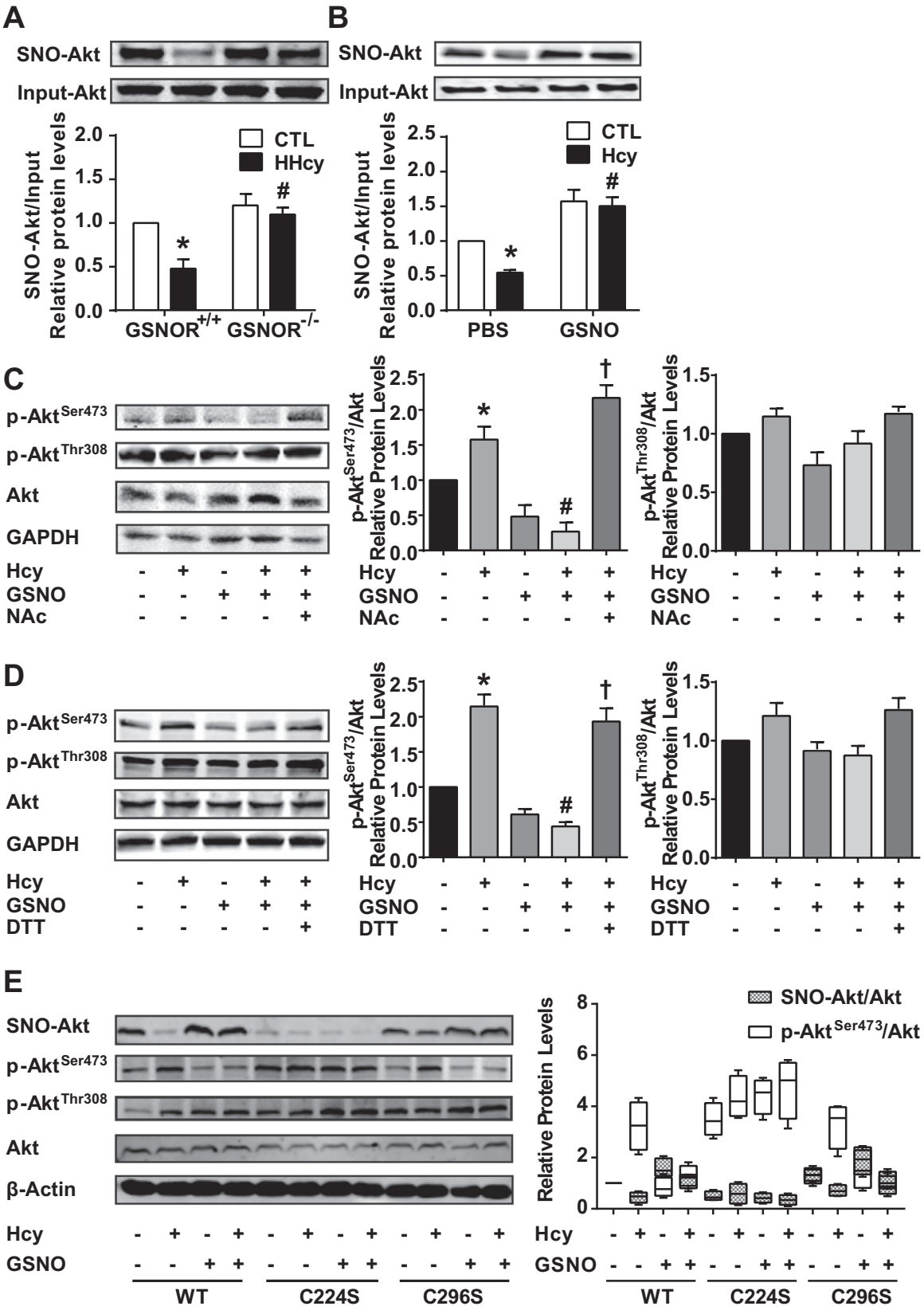

(caption on next page)

reduced upon Hcy stimulation and restored by GSNO treatment, while S-nitrosylated C224S Akt remained low levels among all groups (Fig. 3E). Our results suggest that Cys224 was the major S-nitrosylated residue in Akt, which is consistent with the previous report [26]. Meanwhile, we examined the phosphorylation level in these Akt variants. In contrast to S-nitrosylation, phosphorylated Ser473 was elevated and reversed by Hcy and GSNO treatment, respectively, in wild-type and C296S Akt. And phosphorylation of C224S Akt at Ser473

Fig. 3. S-nitrosylation of Akt at Cys224 inhibits the phosphorylation of Akt at Ser473. (*A-B*), S-nitrosylation of Akt (SNO-Akt) in T cells examined by biotin switch assay *in vivo* (*A*) or *in vitro* (*B*). (*C-D*), Phosphorylation of Akt detected by western blot analysis in T cells purified from C57BL/6 J mice, in which isolated T cells were cultured with plate-bound anti-CD3 antibody and pretreated for 30 min with or without 50 μmol/L GSNO or the indicated S-nitrosylation inhibitor, 50 μmol/L N-acetyl-L-cysteine (NAc) (*C*) or 25 μmol/L dithiothreitol (DTT) (*D*), then incubated with or without 100 μmol/L Hcy for 24 h. (*E*), EL4 cells were transiently transfected with flag-labeled wild-type (WT) and mutated Akt (C224S or C296S). At 24 h after transfection, EL4 cells expressing Akt variants were pretreated for 30 min with or without 100 μmol/L GSNO, then incubated with or without 100 μmol/L Hcy for 24 h. S-nitrosylation of flag-labeled Akt was detected by biotin switch assay. Phosphorylation of flag-labeled Akt at Ser473 and Thr308 measured by western blot analysis. Flag-labeled Akt was an internal control. Data are mean ± SEM of at least three independent experiments (n = 3–6 mice in each group). * $P<.05$ compared with the control. # $P<.05$ compared with HHcy or Hcy. † $P<.05$ compared with Hcy + GSNO. n.s. not significant.

remained a significant high level (Fig. 3E). In addition, circular dichroism (CD) spectra for Akt showed two distinct peaks at 222 and 208 nm, which suggests a high content of α-helix (24.07 ± 0.32) in the Akt secondary structure. GSNO-treated Akt caused a significant decrease at both 222 and 208 nm in the CD spectrum, which suggests a lower content of α-helix (22.43 ± 0.81) in S-nitrosylated Akt (Supplementary Fig. 4A-B). Collectively, these results indicate that S-nitrosylation of Akt at Cys224 likely caused the decreased α-helical secondary structure, which might inhibit the phosphorylation of Akt at Ser473.

3.4. GSNOR$^{-/-}$ApoE$^{-/-}$ mice have less activated T cells under HHcy

Accumulating evidence suggests that T-cell activation is critical in HHcy-accelerated atherosclerosis in ApoE$^{-/-}$ mice, particularly during the early stages of the disease [4–7]. Given that GSNOR deficiency or GSNO supplementation prevented Hcy-induced T-cell proliferation and activation, we hypothesized that GSNOR ablation in T cells could attenuate the early development of atherosclerosis. To test this hypothesis, we generated GSNOR$^{-/-}$ApoE$^{-/-}$ double knockout mice and their GSNOR$^{+/+}$ApoE$^{-/-}$ littermates by crossing GSNOR$^{-/-}$ and ApoE$^{-/-}$ mice (Supplementary Fig. 5A-B). Both GSNOR$^{-/-}$ApoE$^{-/-}$ and GSNOR$^{+/+}$ApoE$^{-/-}$ mice were fed Hcy (1.8 g/L) or not in drinking water for 4 weeks. Plasma Hcy concentrations were significantly elevated after Hcy administration, with no alteration in mouse body weights or total cholesterol and triglyceride levels among all groups (Supplementary Table 2). We initially examined the proliferation and activation of T cells in the four groups of mice. HHcy markedly increased the number of splenic T cell (Fig. 4A) and proliferation of CFSE-labeled T cells (Fig. 4B) as well as level of IL-2 and IFN-γ (Fig. 4C-F) in GSNOR$^{+/+}$ApoE$^{-/-}$ mice but only marginally activated T cells in GSNOR$^{-/-}$ApoE$^{-/-}$ mice. The Akt signaling network and Akt activity were suppressed in GSNOR$^{-/-}$ApoE$^{-/-}$ mice as compared with GSNOR$^{+/+}$ApoE$^{-/-}$ littermates (Fig. 4G, H). Consistently, HHcy significantly induced p-Akt^{Ser473} but not p-Akt^{Thr308} in T cells from GSNOR$^{+/+}$ApoE$^{-/-}$ mice with no HHcy induction of p-Akt^{Ser473} in T cells from GSNOR$^{-/-}$ApoE$^{-/-}$ mice (Fig. 4I).

3.5. GSNOR ablation ameliorates HHcy-induced atherosclerosis in ApoE$^{-/-}$ Mice

Because GSNOR$^{-/-}$ApoE$^{-/-}$ mice exhibited much less activation of T cells and Akt signaling in response to HHcy, we then compared the HHcy-accelerated atherosclerosis in GSNOR$^{+/+}$ApoE$^{-/-}$ and GSNOR$^{-/-}$ApoE$^{-/-}$ mice. With Hcy administration, total lesions in the aortic root were significantly less in GSNOR$^{-/-}$ApoE$^{-/-}$ than GSNOR$^{+/+}$ApoE$^{-/-}$ mice (Fig. 5A). In line with the reduced atherosclerosis, the recruitment of the CD68-positive macrophages and CD3-positive T cells to the atherosclerotic lesions was significantly lower in GSNOR$^{-/-}$ApoE$^{-/-}$ than GSNOR$^{+/+}$ApoE$^{-/-}$ mice (Fig. 5B, C). Moreover, the gene expression of HHcy-elevated inflammatory cytokines, including *il-2, ifn-γ, tnf-α and mcp1*, was significantly lower in aortas of GSNOR$^{-/-}$ApoE$^{-/-}$ than GSNOR$^{+/+}$ApoE$^{-/-}$ mice (Fig. 5D). Cytometric bead array analysis showed that plasma levels of inflammatory cytokines, including TNF-α, IFN-γ, and IL-12p70, were lower in GSNOR$^{-/-}$ApoE$^{-/-}$ than GSNOR$^{+/+}$ApoE$^{-/-}$ mice (Fig. 5E). In addition, the level of protein S-nitrosylation was restored in the atherosclerotic plaques in HHcy-administered GSNOR$^{-/-}$ApoE$^{-/-}$ mice, as revealed by immunofluorescent staining (Supplementary Fig. 6), which confirmed that the protein S-nitrosylation was downregulated with Hcy-induced GSNOR in the atherosclerotic plaques during atherogenesis.

3.6. Adoptive transfer of GSNOR$^{-/-}$ T cells decreases HHcy-induced atherosclerosis in ApoE$^{-/-}$ recipient mice

To address the specific role of GSNOR ablation in T cells contributing to the reduced atherosclerosis in GSNOR$^{-/-}$ApoE$^{-/-}$ mice, we used *in vivo* adoptive T-cell transfer into ApoE$^{-/-}$ mice. To deplete T cells first in the recipient ApoE$^{-/-}$ mice, animals were intraperitoneally injected with CD3 blockade antibody to reduce the T-cell number and add space for the injected T cells [28,29]. The proportion of CD3$^+$ T cells in peripheral lymphatic nodes and spleen as well as direct splenic T-cell counts were markedly lower in ApoE$^{-/-}$ mice administered CD3 blockade antibody than the isotype control IgG (Supplementary Fig. 7A-C). The T-cell-depleted ApoE$^{-/-}$ mice then received T cells transferred from GSNOR$^{+/+}$ or GSNOR$^{-/-}$ mice *via* tail vein injection. The two groups were then fed normal chow with or without Hcy in drinking water for another 3 weeks (Fig. 6A). Oil-red O staining showed much increased atherosclerosis in the aorta roots of ApoE$^{-/-}$ mice receiving GSNOR$^{+/+}$ T cells as compared with GSNOR$^{-/-}$ T cells (Fig. 6B). Additionally, the atherosclerotic regions showed more enhanced infiltration of CD68-positive macrophages and CD3-positive T cells in ApoE$^{-/-}$ mice receiving GSNOR$^{+/+}$ than GSNOR$^{-/-}$ T cells (Fig. 6C, D). Together, these data indicate that the HHcy-increased GSNOR in T cells contributed to the early stage of atherogenesis.

3.7. S-Nitrosylation in T cells inversely correlates with plasma Hcy levels in human CAD patients

With the established mechanism by which the GSNOR-activated T cell contributed to atherosclerosis, we next explored the translational implication of this mechanism in the context of human patients. Peripheral blood mononuclear cells (PBMCs) were isolated from 18 patients who underwent coronary artery angiography and were diagnosed with CAD and HHcy (plasma Hcy level above 10 μmol/L). The baseline characteristics of patients are summarized (Supplementary Table 3). The level of *Gsnor* in PBMCs, SNO-Cys mean fluorescence intensity (MFI) and IFN-γ$^+$ subsets of T cells from patients were assessed by RT-PCR and flow cytometry. The mRNA level of *Gsnor* was positively correlated with plasma Hcy concentration (Fig. 7A). Conversely, the level of S-nitrosylation in T cells, indicated by SNO-Cys MFI, was inversely correlated with Hcy concentration (Fig. 7B). Furthermore, the proportion of IFN-γ$^+$ T cells was positively correlated with level of Hcy (Fig. 7C), which suggests that Hcy promoted T-cell activation in humans during the onset of HHcy-related CAD.

In conclusion, these results support that the HHcy-induced GSNOR is a key factor switching Akt S-nitrosylation to phosphorylation in T-cell activation, which in turn acts as a pathophysiological regulator of T-cell-driven atherosclerosis, as schematically illustrated in Fig. 7D.

4. Discussion

HHcy accelerates atherosclerosis, due in part to, HHcy promotion of

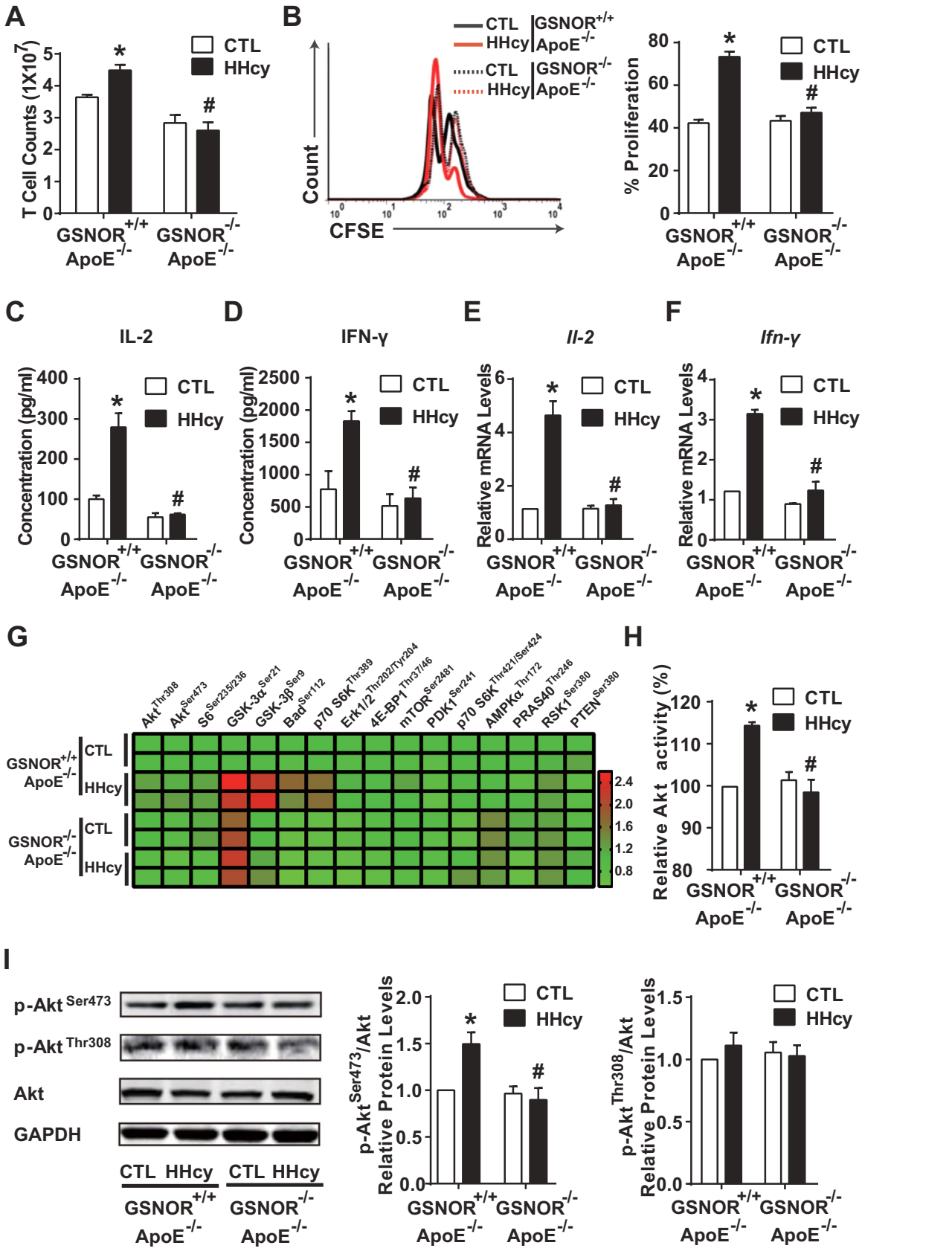

(caption on next page)

Fig. 4. GSNOR$^{-/-}$ApoE$^{-/-}$ mice have less activated T cells under HHcy. GSNOR$^{+/+}$ApoE$^{-/-}$ and GSNOR$^{-/-}$ApoE$^{-/-}$ mice were fed a normal chow diet and given drinking water supplemented with or without 1.8 g/L Hcy for 4 weeks. (*A*), Total cell numbers of splenic T cells were counted. (*B*), Purified T cells were labeled with CFSE before culture with plate-bound anti-CD3 antibody, then cell proliferation was assessed by flow cytometry after 48 h. (*C-D*), Purified T cells were cultured with plate-bound anti-CD3 antibody for an additional 24 h. ELISA of IL-2 (*C*) and IFN-γ (*D*) levels in the supernatants of cultured T cells. (*E-I*), In freshly isolated splenic T cells, gene expression of *Il-2* (*E*) and *Ifn*-γ (*F*) was measured by quantitative PCR. Phosphorylated proteins in Akt signaling networks (*G*) were detected as described in Fig. 2, and Akt kinase enzyme activity (*H*) was analyzed. Phosphorylation levels of Akt at Ser473 and Thr308 (*I*) were detected by western blot analysis. GAPDH was an internal control. Data are the mean ± SEM of at least three independent experiments (n = 3–6 mice in each group). $^{*}P<.05$ compared with the control. $^{\#}P<.05$ compared with HHcy.

T-cell proliferation and secretion of proinflammatory cytokines (IL-2 and IFN-γ) [4–7]. GSNOR reduces cellular levels of protein S-nitrosylation by regulating the equilibrium between GSNO and SNO-proteins [14]. Despite the reported roles of GSNOR in T-cell development and negative selection [11], whether and how GSNOR participates in T-cell activation in terms to HHcy-related atherosclerosis remain largely unknown. Aiming at studying the mechanism by which HHcy induces T-cell activation, we demonstrated significantly increased GSNOR expression in T cells in response to HHcy *in vivo*. GSNOR$^{-/-}$ApoE$^{-/-}$ double knock-out and adoptive transfer of GSNOR$^{-/-}$ T cells into ApoE$^{-/-}$ mouse models showed a reduction in the HHcy-induced T-cell activation and atherosclerosis. The role of GSNOR in the HHcy-induced T-cell activation and T-cell-driven cardiovascular disease were further verified in human CAD patients with HHcy.

The level of S-nitrosylation in T cells should involve systematic regulations among an array of enzymes including NOS and denitrosylases. HHcy would disturb the homeostasis of this regulation in T cells. Our present study shows that Hcy stimulation induced GSNOR expression in T cells *in vitro*, with a marked decline in the overall protein S-nitrosylation levels and no apparent alterations in iNOS and Trx expression. Elevated level of SNOs with an impaired immune system in GSNOR$^{-/-}$ mice [15,36] indicates that such exacerbated accumulation of SNOs may have inhibitory effects on T-cell activation. Consistently, in our study, *gsnor* ablation in GSNOR$^{-/-}$ mice represented an *in vivo* HHcy model, which recapitulated findings from the *in vitro* study showing HHcy-induced T-cell activation suppressed in GSNOR$^{-/-}$ mice. Evidence from these *in vitro* and *in vivo* studies suggest that GSNOR is a major regulator of Hcy-induced denitrosylation in T cells.

The Hcy-Akt signaling axis has been found involved in T-cell activation [21–23,33,37]. For example, Hcy-elicited Akt phosphorylation is linked to the enhanced secretion of proinflammatory cytokines [6]. In accordance with these findings, our study demonstrates that Hcy caused the phosphorylation of Akt at Ser473, and GSNOR deficiency or GSNO supplementation reversed this phosphorylation. Therefore, the HHcy-induced Akt activation in T cells is GSNOR-dependent. S-nitrosylation of Akt in various cell types, including C2C12 myotubes, skeletal cells and esophageal squamous cells, is implicated in the pathogenesis of diabetes, burn injuries and Barrett's esophagus, respectively [25–27]. Given that Hcy activation of Akt is GSNOR-dependent, Akt may be a key target for GSNOR-mediated denitrosylation in T-cell activation. Indeed, our data in Fig. 3 showed that the level of SNO-Akt in T cells was lower, along with T-cell activation on HHcy stimulation. In terms of the underlying mechanism, we showed that GSNOR-dependent Akt denitrosylation was associated with increased Akt activity and Akt phosphorylation, in particular, at Ser473.

The crosstalk between S-nitrosylation and other post-translational modifications such as phosphorylation, ubiquitination and acetylation has been extensively studied [38]. In our study, GSNO exerted an inhibitory effect on the Hcy-induced phosphorylation of Akt at Ser473, which could be restored by the S-nitrosylation inhibitors NAc and DTT. Conserved Cys residues within 8 Å to annotated active sites of Akt1 (*i.e.,* 179 K, 274D) are Cys224, Cys296 and Cys310, as indicated by using PyMOL software. The two reported S-nitrosylation sites of Akt, namely, Cys224 and Cys296 [25,26], were mutated with Ser in our study. In accordance with Kaneki *et al.* findings [26], we showed that Cys224 but not Cys296 was the putative residue for S-nitrosylation. However, by using nano-LC interfaced with tandem quadrupole time-of-flight mass spectrometry (Q-TOF)^{micro} tandem mass spectrometry, Fischman *et al.* showed that S-nitrosylation at Cys296 accelerates its interaction with Cys310 to form a disulfide bond, thus leading to the dephosphorylation at Thr308 [25]. One possible explanation for the lack of S-nitrosylation at Akt Cys296 in our study was the transient existence of S-nitrosylated Cys296, which had switched to a disulfide bond with Cys310 by the time of detection. Instead, our results revealed that S-nitrosylated Cys224 of Akt impaired Akt phosphorylation at Ser473. As previously reported [39], Akt activation by phosphorylation at Ser473 requires a disorder to order transition of α-helix to reconstruct the activation segments. Consistently, our CD spectra for Akt revealed S-nitrosylated Cys224 with decreased α-helical content, so a less-ordered α-helix conformation might interfere with phosphorylation of Ser473. However, further investigations are needed to confirm the exact molecular structural changes in Akt.

We addressed the role of GSNOR-mediated T-cell activation in HHcy-accelerated atherosclerosis *in vivo* by two mouse models. Generated for the first time, GSNOR$^{-/-}$ApoE$^{-/-}$ double knock-out mice showed decreased atherosclerosis in aortic roots in response to HHcy. The specificity of GSNOR ablation in T cells contributing to the decreased atherosclerosis was further verified by the T-cell adoptive transfer experiments. In addition to T cells, other cell types may participate in the amelioration of atherosclerosis in GSNOR$^{-/-}$ApoE$^{-/-}$ mice. The role of HHcy-initiated endothelial cell dysfunction and inflammatory monocyte generation and differentiation during atherogenesis was well established by Wang *et al.* [40–42] Ablation of GSNOR in these cell types may imbalance the protein S-nitrosylation levels and commit to the development of atherosclerosis. As evidenced by recent studies from Liu *et al.*, [8,9] HHcy reduces the level of protein S-nitrosylation in vascular endothelial cells during HHcy-induced atherosclerosis, and supplementation with the NO donor NONOate could reverse the atherosclerosis.

The relevance of GSNOR in HHcy-induced cardiovascular disease was demonstrated by the findings in human CAD patients with HHcy. The level of plasma Hcy was positively correlated with PBMC *Gsnor* expression and IFN-γ-producing T cells but inversely with S-nitrosylation level in T cells, which indicates a proinflammatory role of GSNOR in human T cells. These findings were consistent with the elevated GSNOR level found in human asthmatic lungs and reduced lung inflammatory responses induced by the GSNOR inhibitor SPL-334 [43]. The signaling pathway downstream of GSNOR in human T cells from CAD patients should include activation of Akt, which remains to be verified. These translational studies suggest that GSNOR can be an indicator of vascular disease.

Collectively, our study reveals that GSNOR plays a crucial role in HHcy-induced T-cell activation and atherosclerosis by switching Akt S-nitrosylation to phosphorylation. GSNOR may be a potential therapeutic target for HHcy-induced atherosclerosis and other T-cell-involved inflammatory diseases.

Acknowledgments

We thank Dr. Limin Liu (University of California, San Francisco) for providing the GSNOR$^{-/-}$ mice, Prof. John Y.-J. Shyy (University of California, San Diego) for revising the manuscript, and Prof. Chu Wang and Dr. Nan Chen (Peking University) for Akt structural analysis. The

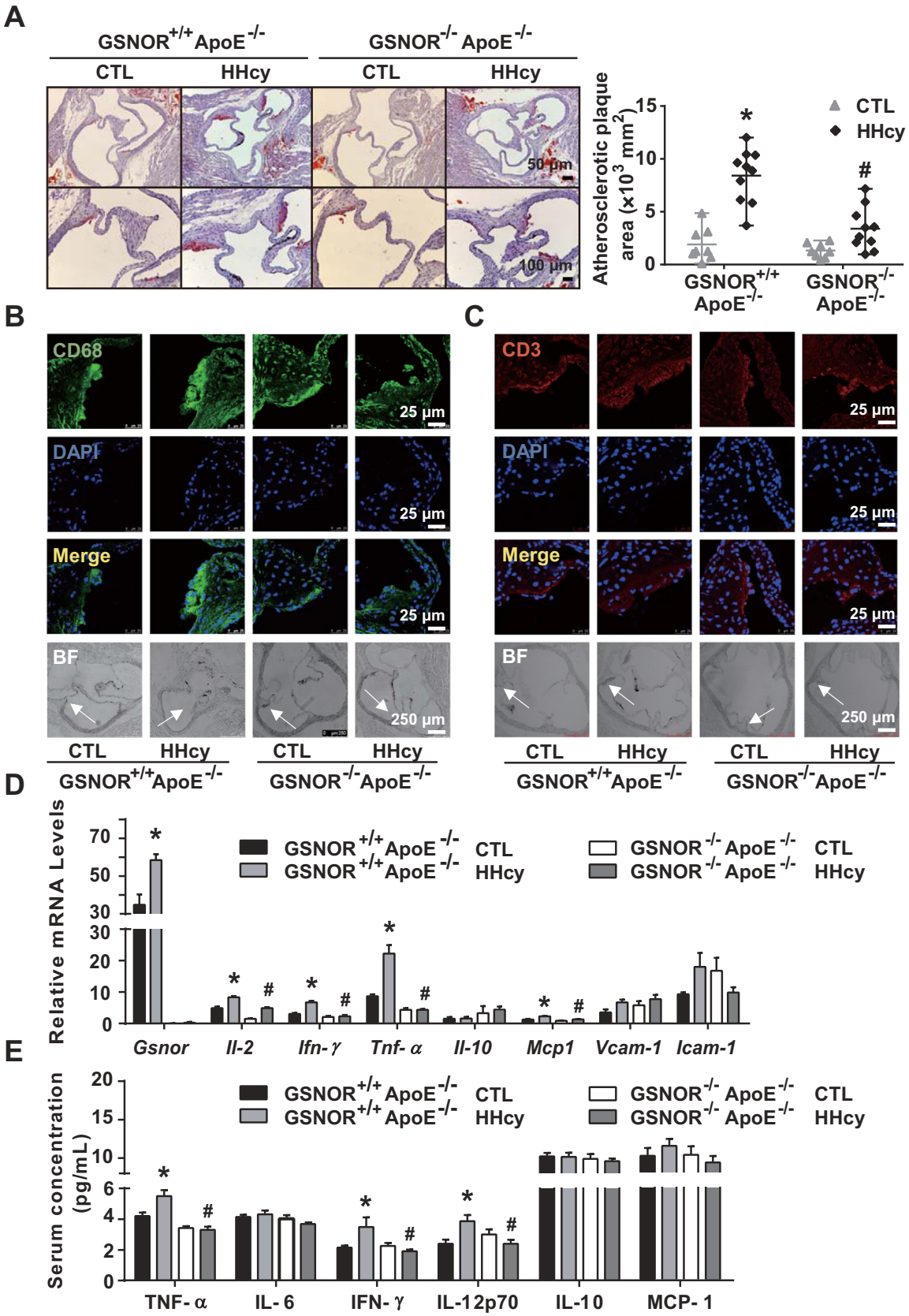

Fig. 5. GSNOR$^{-/-}$ApoE$^{-/-}$ mice show ameliorated HHcy-accelerated atherosclerosis. GSNOR$^{+/+}$ApoE$^{-/-}$ and GSNOR$^{-/-}$ApoE$^{-/-}$ mice were fed a normal chow diet and drinking water supplemented with or without 1.8 g/L Hcy for 4 weeks. (*A*), Oil-red O staining of aortic roots (left panel) and quantification of mean atherosclerotic lesion areas (right panel) are shown. (*B-C*), Representative fluorescence confocal images of infiltration of macrophages (stained with anti-CD68, green) (*B*) and T cells (stained with anti-CD3, red) (*C*) in lesion areas. (*D*), Gene expression of *Gsnor*, *Il-2*, *Ifn-γ*, *Tnf-α*, *Il-10*, *Mcp-1*, *Vcam-1* and *Icam-1* in thoracic aortas isolated from mice measured by quantitative PCR. (*E*), Plasma levels of TNF-α, IL-6, IFN-γ, IL-12p70, IL-10 and MCP-1 detected by cytometric bead array analysis. Data are mean ± SEM of at least three independent experiments (n = 8–10 mice in each group). * P<.05 compared with the control. $^{\#}P$<.05 compared with HHcy.

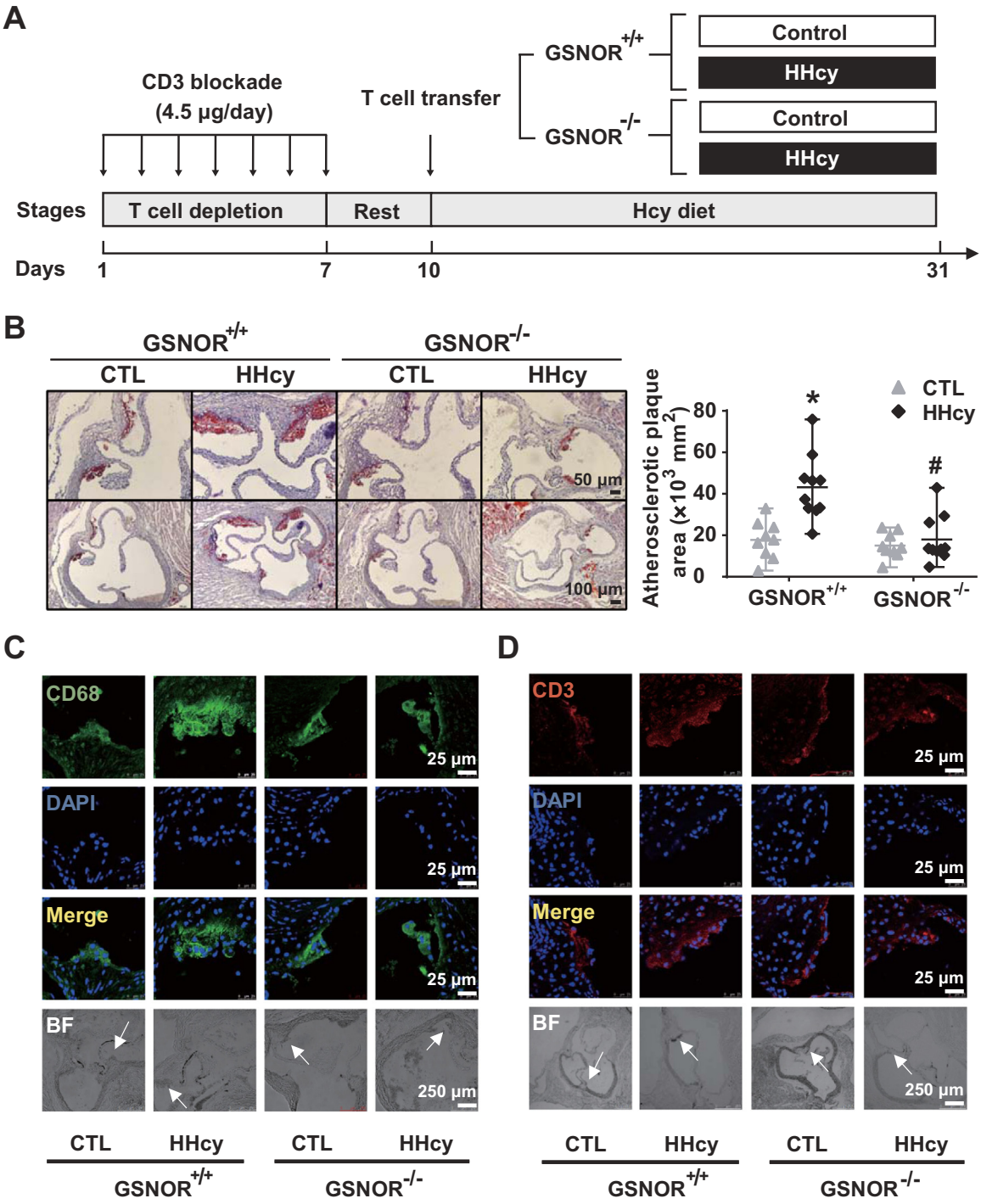

Fig. 6. Adoptive transfer of GSNOR$^{-/-}$ T cells decreases the HHcy-induced atherosclerosis in ApoE-/- recipient mice. (*A*), Schematic flowchart of T cell transfer procedures and induction of HHcy models in recipient ApoE$^{-/-}$ mice. (*B*), Oil-red O staining of aortic roots (left panel) from the recipient mice. Quantification of the mean atherosclerotic lesion areas (right panel). (*C-D*), Representative fluorescence confocal images of infiltration of macrophages (stained with anti-CD68, green) (*C*) and T cells (stained with anti-CD3, red) (*D*) in lesion areas. Data are mean ± SEM of at least three independent experiments (n = 9–10 mice in each group). * P<.05 compared with the control. $^{\#}P$<.05 compared with HHcy.

Figure was partly generated by using Servier Medical Art, provided by Servier, licensed under a Creative Commons Attribution 3.0 unported license (available at http://smart.servier.com).

Conflict of interest

None declared.

Funding

This work was supported by the National Natural Science Foundation of P. R. China (91439206; 81770445; 31570857; 31225012), the National Key Research and Development Program of China (2017YFA0504000, 2016YFC0903100), the Personalized Medicines-Molecular Signature-based Drug Discovery and Development, the Strategic Priority Research Program of the Chinese

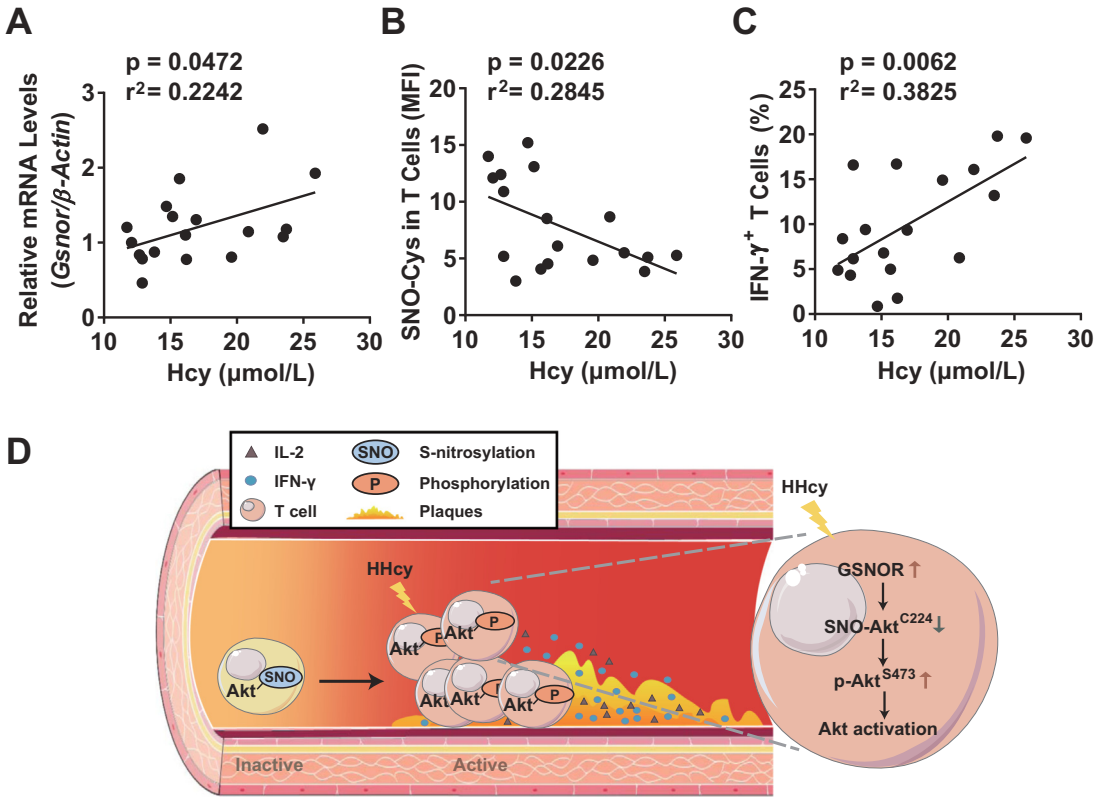

Fig. 7. S-nitrosylation in T cells is inversely correlated with plasma Hcy levels in human CAD patients. Peripheral blood mononuclear cells (PBMCs) from CAD patients with HHcy (above 10 μmol/L) were isolated, collected and stained with anti-CD3, anti-SNO-Cys and anti-IFN-γ antibodies (n = 18). The level of *Gsnor* in PBMCs, the SNO-Cys mean fluorescence intensity (MFI) and IFN-γ^+ subsets of $CD3^+$-gated T cells were assessed by RT-PCR and flow cytometry. (*A-C*), Correlations between the plasma Hcy concentration and *Gsnor* gene expression in PBMCs (*A*), SNO-Cys MFI in T cells (*B*), and IFN-γ^+ T cell percentage (*C*). (*D*), Schematic representation of the proposed mechanism of GSNOR-Akt-dependent T-cell activation in HHcy-induced atherosclerosis. Akt was abundantly S-nitrosylated at Cys224 during inactivation of T cells. On HHcy stimulation, elevated GSNOR denitrosylated Akt and led to Akt phosphorylation at Ser473 with activated Akt signaling pathways, which promoted T-cell proliferation and secretion of proinflammatory cytokines, including IL-2 and IFN-γ. These events were associated with aggravating vascular immune inflammation and early atherosclerotic development, which suggests an essential switch role for the GSNOR-Akt axis dependent denitrosylation in T cell-driven atherosclerosis.

Academy of Sciences (XDA12020316), and Special Program of Peking University for Clinical Medicine + X (PKU2017LCX09).

Author contribution

J.L., J.F., X.W., and C.C. designed and supervised the research; J.L. performed the research, analyzed data, made the figures and wrote the manuscript; Yuying Zhang, S.L., Y.M., J.Y., S.H., X.M., L.H., J.D., and B.L. participated in experiments; Yan Zhang, F.F., and Y.H. assisted in the research; Q.X. provided advice.

Appendix A. Supplementary material

Supplementary data associated with this article can be found in the online version at http://dx.doi.org/10.1016/j.redox.2018.04.021.

References

[1] R. Clarke, L. Daly, K. Robinson, E. Naughten, S. Cahalane, B. Fowler, I. Graham, Hyperhomocysteinemia: an independent risk factor for vascular disease, N. Engl. J. Med 324 (1991) 1149–1155.
[2] J.W. Eikelboom, E. Lonn, J. Genest Jr, G. Hankey, S. Yusuf, Homocyst(e)ine and cardiovascular disease: a critical review of the epidemiologic evidence, Ann. Intern Med 131 (1999) 363–375.
[3] K.S. McCully, Homocysteine and vascular disease, Nat. Med 2 (1996) 386–389.
[4] J. Dai, W. Li, L. Chang, Z. Zhang, C. Tang, N. Wang, Y. Zhu, X. Wang, Role of redox factor-1 in hyperhomocysteinemia-accelerated atherosclerosis, Free Radic. Biol. Med 41 (2006) 1566–1577.
[5] Q. Zhang, X. Zeng, J. Guo, X. Wang, Oxidant stress mechanism of homocysteine potentiating Con A-induced proliferation in murine splenic T lymphocytes, Cardiovasc Res 53 (2002) 1035–1042.
[6] K. Ma, S. Lv, B. Liu, Z. Liu, Y. Luo, W. Kong, Q. Xu, J. Feng, X. Wang, CTLA4-IgG ameliorates homocysteine-accelerated atherosclerosis by inhibiting T-cell over-activation in apoE(-/-) mice, Cardiovasc Res 97 (2013) 349–359.
[7] J. Feng, Z. Zhang, W. Kong, B. Liu, Q. Xu, X. Wang, Regulatory T cells ameliorate hyperhomocysteinaemia-accelerated atherosclerosis in apoE-/- mice, Cardiovasc Res 84 (2009) 155–163.
[8] Y. Chen, R. Liu, G. Zhang, Q. Yu, M. Jia, C. Zheng, Y. Wang, C. Xu, Y. Zhang, E. Liu, Hypercysteinemia promotes atherosclerosis by reducing protein S-nitrosylation, Biomed. Pharmacother. 70 (2015) 253–259.
[9] Y. Chen, S. Zhao, Y. Wang, Y. Li, L. Bai, R. Liu, J. Fan, E. Liu, Homocysteine reduces protein S-nitrosylation in endothelium, Int J. Mol. Med 34 (2014) 1277–1285.
[10] N.T. Moldogazieva, I.M. Mokhosoev, N.B. Feldman, S.V. Lutsenko, ROS and RNS signaling: adaptive redox switches through oxidative/nitrosative protein modifications, Free Radic. Res (2018) 1–771.
[11] P. Hernansanz-Agustin, A. Izquierdo-Alvarez, A. Garcia-Ortiz, S. Ibiza, J.M. Serrador, A. Martinez-Ruiz, Nitrosothiols in the immune system: signaling and protection, Antioxid. Redox Signal 18 (2013) 288–308.
[12] S. Duan, C. Chen, S-nitrosylation/denitrosylation and apoptosis of immune cells, Cell Mol. Immunol. 4 (2007) 353–358.
[13] M.W. Foster, T.J. McMahon, J.S. Stamler, S-nitrosylation in health and disease, Trends Mol. Med 9 (2003) 160–168.
[14] L. Liu, A. Hausladen, M. Zeng, L. Que, J. Heitman, J.S. Stamler, A metabolic enzyme for S-nitrosothiol conserved from bacteria to humans, Nature 410 (2001) 490–494.
[15] Z. Yang, Z.E. Wang, P.T. Doulias, W. Wei, H. Ischiropoulos, R.M. Locksley, L. Liu, Lymphocyte development requires S-nitrosoglutathione reductase, J. Immunol. 185 (2010) 6664–6669.
[16] J.B. Mannick, A. Hausladen, L. Liu, D.T. Hess, M. Zeng, Q.X. Miao, L.S. Kane, A.J. Gow, J.S. Stamler, Fas-induced caspase denitrosylation, Science 284 (1999) 651–654.
[17] H.E. Marshall, J.S. Stamler, Nitrosative stress-induced apoptosis through inhibition of NF-kappa B, J. Biol. Chem. 277 (2002) 34223–34228.
[18] B. Zech, R. Kohl, A. von Knethen, B. Brune, Nitric oxide donors inhibit formation of the Apaf-1/caspase-9 apoptosome and activation of caspases, Biochem J. 371 (2003) 1055–1064.

[19] N. Azad, V. Vallyathan, L. Wang, V. Tantishaiyakul, C. Stehlik, S.S. Leonard, Y. Rojanasakul, S-nitrosylation of Bcl-2 inhibits its ubiquitin-proteasomal degradation. A novel antiapoptotic mechanism that suppresses apoptosis, J. Biol. Chem. 281 (2006) 34124–34134.
[20] M. Vig, S. Srivastava, U. Kandpal, H. Sade, V. Lewis, A. Sarin, A. George, V. Bal, J.M. Durdik, S. Rath, Inducible nitric oxide synthase in T cells regulates T cell death and immune memory, J. Clin. Invest 113 (2004) 1734–1742.
[21] J. Song, F.T. Lei, X. Xiong, R. Haque, Intracellular signals of T cell costimulation, Cell Mol. Immunol. 5 (2008) 239–247.
[22] B. Bauer, G. Baier, Protein kinase C and AKT/protein kinase B in CD4+ T-lymphocytes: new partners in TCR/CD28 signal integration, Mol. Immunol. 38 (2002) 1087–1099.
[23] D. Cantrell, Protein kinase B (Akt) regulation and function in T lymphocytes, Semin Immunol. 14 (2002) 19–26.
[24] G.K. Hansson, A. Hermansson, The immune system in atherosclerosis, Nat. Immunol. 12 (2011) 204–212.
[25] X.M. Lu, R.G. Tompkins, A.J. Fischman, Nitric oxide activates intradomain disulfide bond formation in the kinase loop of Akt1/PKB alpha after burn injury, Int. J. Mol. Med. 31 (2013) 740–750.
[26] T. Yasukawa, E. Tokunaga, H. Ota, H. Sugita, J.A. Martyn, M. Kaneki, S-nitrosylation-dependent inactivation of Akt/protein kinase B in insulin resistance, J. Biol. Chem. 280 (2005) 7511–7518.
[27] K. Asanuma, X. Huo, A. Agoston, X. Zhang, C. Yu, E. Cheng, Q. Zhang, K.B. Dunbar, T.H. Pham, D.H. Wang, K. Iijima, T. Shimosegawa, R.D. Odze, S.J. Spechler, R.F. Souza, In oesophageal squamous cells, nitric oxide causes S-nitrosylation of Akt and blocks SOX2 (sex determining region Y-box 2) expression, Gut 65 (2016) 1416–1426.
[28] R. Hirsch, M. Eckhaus, H. Auchincloss Jr, D.H. Sachs, J.A. Bluestone, Effects of in vivo administration of anti-T3 monoclonal antibody on T cell function in mice. I. immunosuppression of transplantation responses, J. Immunol. 140 (1988) 3766–3772.
[29] S. Steffens, F. Burger, G. Pelli, Y. Dean, G. Elson, M. Kosco-Vilbois, L. Chatenoud, F. Mach, Short-term treatment with anti-CD3 antibody reduces the development and progression of atherosclerosis in mice, Circulation 114 (2006) 1977–1984.
[30] B. Huang, C. Chen, Detection of protein S-nitrosation using irreversible biotinylation procedures (IBP), Free Radic. Biol. Med 49 (2010) 447–456.
[31] S.R. Jaffrey, S.H. Snyder, The biotin switch method for the detection of S-nitrosylated proteins, Sci. STKE 2001 (2001) pl1.
[32] Z. Qu, F.J. Meng, R.D. Bomgarden, R.I. Viner, J.L. Li, J.C. Rogers, J.L. Cheng, C.M. Greenlief, J.K. Cui, D.B. Lubahn, G.Y. Sun, Z.Z. Gu, Proteomic Quantification and Site-Mapping of S-Nitrosylated Proteins Using Isobaric iodoTMT Reagents, J. Proteome Res. 13 (2014) 3200–3211.
[33] T. Saito, T. Yokosuka, A. Hashimoto-Tane, Dynamic regulation of T cell activation and co-stimulation through TCR-microclusters, FEBS Lett. 584 (2010) 4865–4871.
[34] B.D. Manning, A. Toker, AKT/PKB signaling: navigating the network, Cell 169 (2017) 381–405.
[35] I. Hers, E.E. Vincent, J.M. Tavare, Akt signalling in health and disease, Cell Signal 23 (2011) 1515–1527.
[36] L. Liu, Y. Yan, M. Zeng, J. Zhang, M.A. Hanes, G. Ahearn, T.J. McMahon, T. Dickfeld, H.E. Marshall, L.G. Que, J.S. Stamler, Essential roles of S-nitrosothiols in vascular homeostasis and endotoxic shock, Cell 116 (2004) 617–628.
[37] T. Yokosuka, T. Saito, Dynamic regulation of T-cell costimulation through TCR-CD28 microclusters, Immunol. Rev. 229 (2009) 27–40.
[38] S.M. Haldar, J.S. Stamler, S-nitrosylation: integrator of cardiovascular performance and oxygen delivery, J. Clin. Invest 123 (2013) 101–110.
[39] J. Yang, P. Cron, V. Thompson, V.M. Good, D. Hess, B.A. Hemmings, D. Barford, Molecular mechanism for the regulation of protein kinase B/Akt by hydrophobic motif phosphorylation, Mol. Cell 9 (2002) 1227–1240.
[40] H. Xi, Y. Zhang, Y. Xu, W.Y. Yang, X. Jiang, X. Sha, X. Cheng, J. Wang, X. Qin, J. Yu, Y. Ji, X. Yang, H. Wang, Caspase-1 Inflammasome Activation Mediates Homocysteine-Induced Pyrop-Apoptosis in Endothelial Cells, Circ. Res 118 (2016) 1525–1539.
[41] D. Zhang, X. Jiang, P. Fang, Y. Yan, J. Song, S. Gupta, A.I. Schafer, W. Durante, W.D. Kruger, X. Yang, H. Wang, Hyperhomocysteinemia promotes inflammatory monocyte generation and accelerates atherosclerosis in transgenic cystathionine beta-synthase-deficient mice, Circulation 120 (2009) 1893–1902.
[42] D. Zhang, P. Fang, X. Jiang, J. Nelson, J.K. Moore, W.D. Kruger, R.M. Berretta, S.R. Houser, X. Yang, H. Wang, Severe hyperhomocysteinemia promotes bone marrow-derived and resident inflammatory monocyte differentiation and atherosclerosis in LDLr/CBS-deficient mice, Circ. Res 111 (2012) 37–49.
[43] M.E. Ferrini, B.J. Simons, D.J. Bassett, M.O. Bradley, K. Roberts, Z. Jaffar, S-nitrosoglutathione reductase inhibition regulates allergen-induced lung inflammation and airway hyperreactivity, PLoS One 8 (2013) e70351.